

Erik Miller
Jonathan P. Rothstein

Control of the sharkskin instability in the extrusion of polymer melts using induced temperature gradients

Received: 11 February 2004
Accepted: 21 May 2004
Published online: 28 July 2004
© Springer-Verlag 2004

Abstract The extrusion of polymer melts is often rate limited by the onset of an elastic surface instability known as sharkskin. Appearance of these surface distortions is generally unacceptable for commercial applications. The desire to forestall the onset of sharkskin to higher output rates has motivated a considerable amount of research to characterize the nature of the instability. In this manuscript, we will present a series of detailed experiments using a custom fabricated extruder and die. By incorporating thermal breaks and precise localized temperature control of the die and barrel, predetermined temperature gradients could be induced across the extrudate. Polymers are typically very poor thermal conductors, and therefore the effects of heating or cooling from a boundary can be designed to only affect the properties of the extrudate very close to the die wall. We will present data correlating the amplitude and frequency of the sharkskin instability to the bulk and die surface temperature as well as the shear rates. The result is a quantitative

processing map that characterizes the instability and demonstrates that by modifying the rheology of the polymeric fluid very near the die exit corner, it is possible to suppress or control the sharkskin instability through isolated die heating or cooling. By reformulating our data into Weissenberg and Deborah numbers using the relaxation time evaluated at the wall temperature, we demonstrate that the sharkskin surface instability is dependent only on flow kinematics and viscometric properties of the fluid very near the die wall, a result of the stress singularity present at the die exit, and independent of bulk fluid properties. This technique could conceivably increase the profitability of extrusion processes and be extended to develop precisely-controlled sharkskin for designing specific functionality into extruded surfaces.

Keywords Polyethylene extrusion · Sharkskin · Surface instability · Quantitative characterization

E. Miller · J. P. Rothstein (✉)
Department of Mechanical Engineering,
University of Massachusetts, Amherst,
MA 01003-2210, USA
E-mail: rothstein@ecs.umass.edu

Introduction

Flow instabilities occur in a variety of commercial polymer processing operations including extrusion, film blowing, fiber spinning and coating. During the extru-

sion of molten polymer through capillary or slit die geometries, a transition from a smooth surface to a nearly periodic ridge-like surface distortion has been observed at a critical shear rate or wall shear stress (Petrie and Denn 1976; Denn 2001). These surface

distortions are known as sharkskin. Flow instabilities during extrusion were first observed after World War II, and early reports of sharkskin, in particular, date back to the 1960s (Howells and Benbow 1962; Tordella 1963). Detailed experimental observations on flow instabilities through 1975 are reviewed in a broad sense by Petrie and Denn (1976), and subsequently by Larson (1992). A more specific review of flow instabilities, with a focus on sharkskin and its mechanism was written by Denn (2001). In general, and as detailed in the aforementioned reviews, distortions seen during extrusion have a progression in severity. As shear rate or stress increases, the extrudate surface undergoes a transition from stable, to sharkskin, to stick-slip, and finally to gross melt fracture. In Fig. 1, a series of photographs are shown to illustrate the transition from smooth, to loss of gloss, to fully developed sharkskin.

While a great deal of research has been devoted to sharkskin in polymer extrusion, the origins and underlying physical mechanism of this elastic instability are still widely debated within the literature. There is, however, a consensus among researchers that the underlying physical mechanism of the sharkskin instability is rooted in the stress singularity that develops at the die exit. As seen schematically in Fig. 2, large local stresses can develop within the polymer melt near the die exit. This occurs as the fluid accelerates from rest for the case of a no-slip velocity boundary condition, or from a small velocity ($v_{\text{slip}} \ll 1$ mm/s, Denn 2001) for the case of a slip boundary condition to a consistent velocity plug flow beyond the exit plane. The presence of this stress singularity can lead to a rapid tensile deformation of the polymer molecules in the extrudate near the die wall, which can, in turn, result in enormous tensile stresses. The first detailed analysis of this flow and the resulting instability was performed by Cogswell (1977).

The underlying cause of the sharkskin instability is not agreed upon in the literature. Barone et al (1998) proposed an interfacial molecular instability (IMI) mechanism for sharkskin where conditions in the die wall play an important role. In a polymer melt, polymer chains either near to or adsorbed to the die wall are entangled with other chains within the bulk. Near the die exit, if the shear rate is large enough, the stress accumulated within the fluid can grow large enough to result in a coil-stretch transition of these molecules. The chains near the wall elongate and eventually disentangle from the bulk chains. The original chains, now at a lower stress, recoil, and the cycle repeats. Barone et al (1998) assumed that the wall chains are tethered; the mechanics of this microscopic phenomenon incorporating wall-slip are detailed in Mhetar and Archer (1998).

An alternate physical model proposed by Ramamurthy (1986) attributes sharkskin to a failure of adhesion at the polymer/die interface. This claim is further supported by Kalika and Denn (1987), who described the same

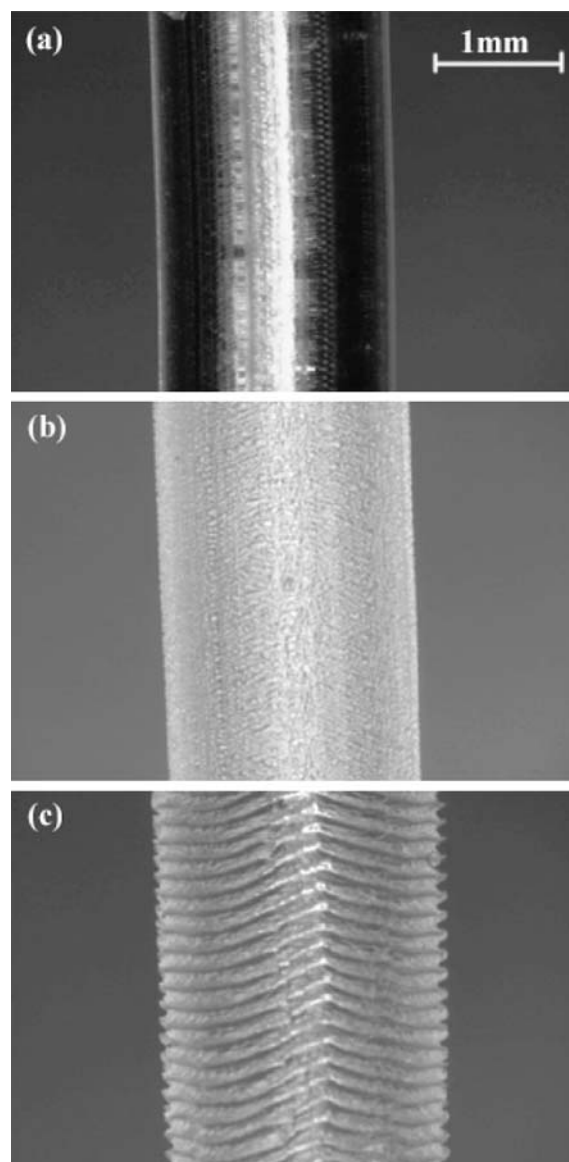


Fig. 1 Series of photographs showing the transition from stable to sharkskin extrudate. From top to bottom: **a** smooth ($\dot{\gamma} = 8 \text{ s}^{-1}$), **b** loss of gloss or onset of sharkskin ($\dot{\gamma} = 16 \text{ s}^{-1}$), and **c** fully developed sharkskin ($\dot{\gamma} = 50 \text{ s}^{-1}$). All photos are from the same experiment using Dow Affinity EG8100 LLDPE, extruded at $T_{\text{bulk}} = 140 \text{ }^\circ\text{C}$

sharkskin mechanism based on periodic slip at the die exit followed by nearly complete slip in the gross melt fracture regime. A later work by El Kissi and Piau (1994), however, directly contradicts the wall slip results in the previous works using the same fluids and a series of capillaries with different geometries. They performed the same flow and rheometry experiments using time-temperature superposition and careful selection of dies and extrusion temperatures rather than extrapolation of data. Their precise results and analysis clearly showed that the experimental methods for determining slip

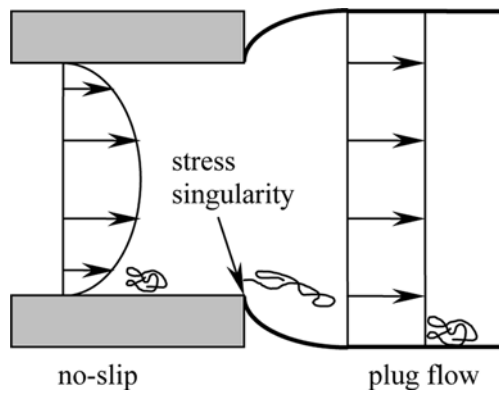


Fig. 2 Schematic diagram of a capillary die exit geometry showing no-slip wall condition and plug flow in the extrudate, with inherent stress singularity. High local stresses at the die exit plane result in strong deformation of the polymer chains and large tensile stresses

velocities do not give conclusive evidence of the existence of slip at the wall for the linear low-density polyethylene (LLDPE) used by Kalika and Denn (1987) and Ramamurthy (1986). El Kissi and Piau (1994) suggested that the slip at the wall reported by the previous authors can, in fact, be attributed to shear thinning, and finally concluded that sharkskin in LLDPE is caused instead by a cracking of the fluid at the die exit. This mechanism is based on the hypothesis that local stresses at the die exit exceed the melt strength and cause a surface melt fracture with a cyclic nature, which is further described by Piau et al (1989) as an exit phenomenon related to the relaxation of stretch strains.

In spite of the continued debate between some of the above works, there is a commonality one can infer about the nature of the sharkskin mechanism. The phenomenon of sharkskin is fundamentally rooted in the kinematics and dynamics of the flow near the capillary die exit and the build-up of tensile stress resulting from the stress singularity. In particular, numerical simulation results by Mackley et al (1998) support this claim and refer to the mechanism as a periodic melt rupture at the die exit resulting from large velocity gradients, deformations and stresses, confined to the surface region. In a more experimental approach by Dhori et al (1997), the effects of the exit corner were explicitly probed. Dies were dipped in a fluoroelastomer additive (Dynamar 9613) known to eliminate sharkskin. The extent of the coating was varied from a few millimeters deep to the entire capillary length. Extruding through these capillaries before coating, after coating, and finally after the coating was machined off the face of the die, only showed sharkskin, suppression of sharkskin, and reappearance, respectively. This careful series of experiments therefore clearly demonstrated that the suppressive coating only affected sharkskin when present at the outermost die exit corner.

Surface quality is important in most extrusion applications. For example, extruded optical fibers must

be free from surface defects if they are to transmit light effectively. Thin fibers that are to be woven into some other final product are difficult to work with if their surfaces are not smooth and able to slide past other fibers easily. Therefore, suppression or elimination and an understanding of sharkskin have practical relevance in that the instability limits the output rate for acceptable extrudate. To this end, there is a large body of previous work that addresses the suppression of sharkskin based on the mechanism described above. Already mentioned above in the work by Dhori et al (1997), coatings which promote slip in the die/polymer interface have been studied extensively. Inn et al (1998) show the effectiveness of a simple soap solution coating around the die exit in eliminating sharkskin for the extrusion of polybutadiene. Previous work has also shown successful suppression or complete elimination of sharkskin in polyethylene extrusion with the use of fluoropolymer polymer processing additives (PPA). In the work of Migler et al (2001), PPA is mixed with the LLDPE resin and, with the aid of a sapphire capillary die, is observed to migrate to the capillary wall where it sticks and induces slip between itself and the LLDPE. The slip velocity at the wall reduces the stress built up at the die exit, thereby postponing or even eliminating sharkskin altogether. Although successful, the addition of PPAs is not always desirable in a final LLDPE product. Rather than using a PPA, experiments by Piau et al (1995) use special stainless steel dies and polytetrafluoroethylene (PTFE or Teflon) inserts. These PTFE inserts or sleeves also eliminate sharkskin without affecting the composition of the product. PTFE inserts are, however, limited in their resistance to high temperature and susceptibility to wear. Alpha brass is another die material shown to induce enough wall slip to suppress sharkskin, as first suggested by Ramamurthy (1986) and later verified by Ghanta et al (1998) and Perez-Gonzalez and Denn (2001).

Rather than addressing the onset of sharkskin by changing the material at the polymer/die interface, our research focuses on affecting the properties of the polymer itself towards the goal of reducing polymeric stress and deformation at the die exit. By using very specific and localized heating/cooling in the die, we will show that it is possible to locally affect the fluid temperature and therefore fluid rheology only near the capillary wall. The rheological properties of polymers are very sensitive in general to small changes in temperature. The theory of time-temperature superposition allows one to relate changes in viscosity and relaxation time to changes in temperature (Bird et al 1987). The Arrhenius form of the time-temperature superposition shift factor is valid for polymer melts far from their melting point and is given by

$$a_T = \frac{\lambda(T)T}{\lambda(T_{\text{ref}})T_{\text{ref}}} = \frac{\eta(T)}{\eta(T_{\text{ref}})} = \exp \left[\frac{\Delta H}{R} \left(\frac{1}{T} - \frac{1}{T_{\text{ref}}} \right) \right] \quad (1)$$

where ΔH is the activation energy, \bar{R} is the universal gas constant, and T_{ref} is an arbitrary reference temperature (Bird et al 1987). Therefore, a strong coupling between flow kinematics and the temperature gradients imposed upon the flow through the thermal boundary conditions (die heating/cooling) can exist. A detailed analytical treatment of flow through capillaries with die heating is presented by Winter (1977). This shift factor, a_T , allows for the creation of master curves of properties such as viscosity from rheology experiments over a wide range of temperatures.

The relatively poor thermal conductivity of polymer melts results in the effects of die heating being isolated to the polymeric fluid near the wall and die exit. The approximate thermal boundary layer thickness, δ_T , can be related to relevant geometric and physical properties of the flow by

$$\frac{\delta_T}{L} \propto \frac{[\alpha \cdot t]^{1/2}}{L} = \left[\frac{\alpha}{\bar{V}L} \right]^{1/2} = Pe^{-1/2} \quad (2)$$

where t is the fluid's residence time in the capillary, L is the capillary length, and \bar{V} is the average velocity. The final scaling argument in Eq. 2 relates the thermal boundary layer thickness, as a fraction of capillary length, to a Peclet number, a dimensionless group which relates the characteristic timescale of thermal diffusion to the characteristic timescale of the flow. Using typical values for average velocity on the order of $\bar{V}=0.01\text{m/s}$, capillary length $L=10\text{ mm}$, and a typical value of thermal diffusivity for LLDPE of $\alpha=1.86 \times 10^{-7}\text{ m}^2/\text{s}$ (Touloukian 1979), gives a result of $Pe=537$ and $\delta_T/L=0.043$. A more meaningful result is attained by multiplying this result by the aspect ratio of our capillary, $L/D=5$, arriving at a final result which indicates that the thermal boundary layer grows to roughly 22% of the capillary diameter, D . In terms of the die heating/cooling experiment, this scaling argument highlights the importance of easily controlled variables such as aspect ratio and average velocity. Extruding through a shorter capillary or at higher flow rates will cause the Peclet number to increase and thereby minimize the growth of the thermal boundary layer even further.

Using the ideas above, let us undertake a brief conceptual exercise. Heating the final section of a capillary die some percent above the bulk working temperature will result in a radial temperature profile in the polymer melt across the plane of the die exit. This profile will vary from some bulk temperature at the centerline to the elevated capillary wall temperature. If the localized heating is designed correctly, the majority of the polymer melt in the resulting temperature distribution will be near the upstream bulk temperature. Consequently, this induced temperature profile will translate into an analogous distribution of the fluid rheology, resulting in a dramatic reduction in both the viscosity and the

relaxation time of the polymeric fluid near the die wall. It is our hypothesis that this local modification of the fluid rheology will directly correspond to a respective increase in a critical output rate before the onset of sharkskin.

In extrusion flows, the polymer melt can be exposed to large shear rates over an extended time. As a result of the poor thermal conductivity of typical polymeric materials, the accumulated heat from viscous dissipation can also have a significant effect on the temperature profile in the extrudate and the viscometric properties of the fluid. The relative importance of viscous heating can be quantified by the Nahme number (Bird et al 1987)

$$Na \equiv \frac{\eta_0 \beta \bar{V}^2}{k_t T} \quad (3)$$

where η_0 is the zero-shear-rate viscosity, k_t is the thermal conductivity of the fluid, T is the absolute temperature, and β is the thermal sensitivity of the fluid viscosity defined as

$$\beta \equiv \frac{T}{\eta_0} \left(\frac{d\eta}{dT} \right) \quad (4)$$

For the Arrhenius form of time-temperature superposition, this simplifies to $\beta = \Delta H/\bar{R}T$. Using $k_t=0.416\text{ W/m}\times\text{K}$ and calculating $\beta=8.38$ at a temperature of $T=413\text{ K}$, gives a relatively small Nahme number of $Na=0.195$ for this flow. It has been shown by Winter (1977) that the effect of viscous heating in an extrusion flow is not to heat the fluid near the die where it would be useful for our purposes, but away from the wall and towards the centerline. The extent of heating and location of the maximum temperature is a strong function of Nahme number and residence time. Viscous heating can have negative effects by raising the temperature of internal regions of the polymer melt above acceptable levels and could result in polymer degradation (Chung 2000).

The strategy of raising temperature to control or eliminate flow instabilities by decreasing viscosity is not altogether new. Industrial practices routinely suggest ramping up temperature through consecutive heating zones in screw-type extruders (Chung 2000; Michaeli 1984). The opposite approach, die cooling, has also been suggested in a British patent by Cogswell (1976), in which he suggests that sharkskin occurs at a given temperature, and can be avoided by cooling the surface of the extrudate as it exits the die. Work by Santamaria et al (2003) details how cooling of the die lip to just above the melting point eliminates sharkskin in polyethylene by inducing ordering of the molecules, thereby increasing cohesiveness and reducing the tendency to tear and cause sharkskin. Using a Teflon gap, a large heat sink, and, in some cases, water cooling at the die exit, Barone et al (1998) were able to demonstrate a correlation between the period of the sharkskin instability and the die wall exit temperature. Specifically,

they found that at a given flow rate, the period increases with decreasing die temperature. The experiments of Barone et al (1998) are quite limited in scope and no measurements of the extrudate temperature profile were made. It is therefore uncertain that the observed shift in the sharkskin period is not simply a result of increased bulk temperature of the extrudate. With respect to all the previous research, our approach to die heating/cooling will utilize a very precise experimental design to locally affect the extrudate at the die exit allowing us to not only suppress sharkskin, but also quantify its characteristics and eventually control and predict it. Our results build upon the conclusions of several aforementioned works and add support to the proposed mechanisms for the instability. The practical relevance of our work points to an extrusion method that uses a small amount of added energy in the form of localized die heating to increase output while minimizing necessary bulk temperatures and subsequent cooling times.

The outline of this paper is as follows. In the following section we discuss our experimental setup, fluid rheology, and test protocol. In the next section we present our results demonstrating suppression and control of sharkskin through localized thermal modifications. Finally, we conclude with some implications and suggestions for the use of our technique for industrial extrusion.

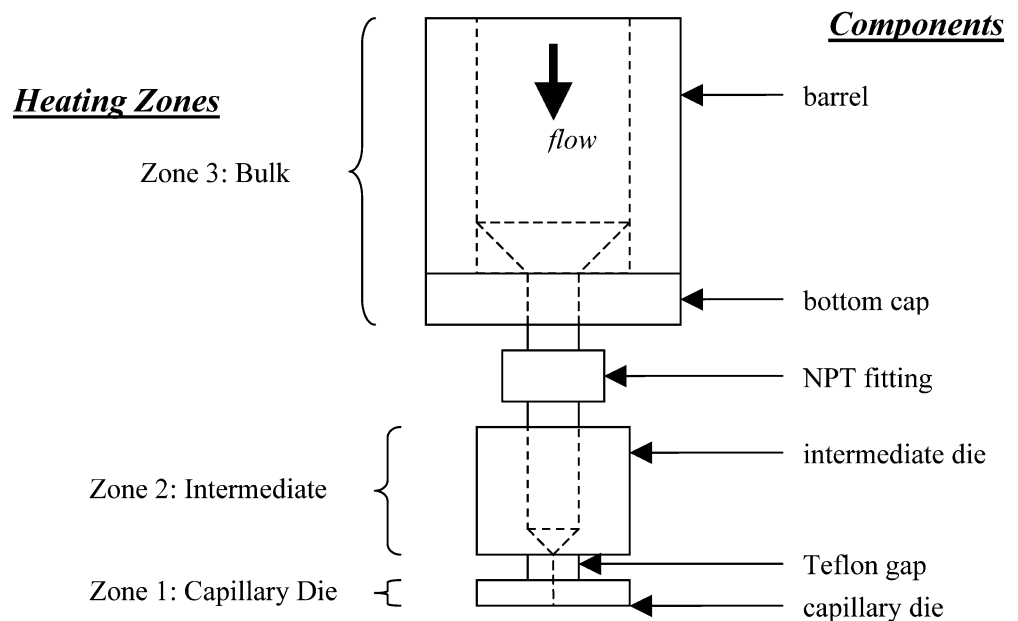
Experimental

Apparatus

A series of experiments were carried out using a purpose-built extruder. In Fig. 3, a schematic diagram of

our experimental set-up is shown, highlighting several key components and heating zones. The barrel, with a 30 mm internal diameter and total volume of 0.19 m^3 , was machined from 7075 aluminum and heated by three 500 W band heaters (Omega MB-1). The temperature of the bulk fluid inside the barrel (Zone 3) is monitored by an internal bore thermocouple (Omega BT) inserted through a radial pressure fitting near the bottom of the barrel. A standard pipe fitting provides the attachment point for the intermediate and capillary die, both constructed of stainless steel and heated by a 100 W band heater (Omega MB-1) and 15 W cartridge heater (Omega CSS-01115), respectively. In the intermediate die (Zone 2), the bulk temperature of the fluid is again monitored by an internal bore thermocouple. However, in the capillary die (Zone 1), rather than controlling the fluid temperature, the temperature of the die itself is monitored for control using a thermocouple mounted directly in contact with the surface of the steel die. A divider fabricated from Teflon provides thermal isolation to the small capillary die. Temperature differences of $\Delta T > 30 \text{ }^\circ\text{C}$ are possible between the capillary and intermediate die. The actual capillary section begins in the intermediate die and is bored smoothly through the 3 mm thick Teflon gap and the 5 mm capillary die. Total length is 10 mm and diameter is 2 mm ($L/D = 5$). All three heating zones are controlled individually by standard proportional-integral controllers (Omega CN2110). Polymer melt is forced out of the barrel and through the die using pressurized nitrogen supplied with a standard compressed nitrogen tank and regulator capable of producing $1.4 \times 10^7 \text{ Pa}$. The regulated pressure is monitored by a 100 mV transducer (Omega PX302) mounted inline at the top of the barrel.

Fig. 3 Schematic diagram of experimental extruder



Working material

The material under investigation is a polyolefin plastomer; specifically, a co-polymer of ethylene and octene. Dow AFFINITY EG8100 was chosen on the basis of being a well-stabilized and commercially-available linear low-density polyethylene (LLDPE), as described in Migler et al (2001). The density of this polymer is $\rho = 870 \text{ kg/m}^3$, and it has a differential scanning calorimeter (DSC) melting point of $T_{\text{melt}} = 55 \text{ }^\circ\text{C}$. EG8100 was delivered in pellet form and in the absence of any instability is transparent. Dynamic and steady flow rheology experiments were performed on this material using parallel plate geometry on an AR2000 shear rheometer (TA Instruments), the results of which are shown in Fig. 4 and Fig. 5, respectively. The small amplitude oscillatory data in Fig. 4 were fit using a discrete multi-mode Maxwell spectrum (Bird et al 1987). In this linear viscoelastic model, the discrete forms of the loss and storage moduli, G' and G'' , respectively, are defined as

$$G' = \sum_{i=1}^n \frac{\eta_i \lambda_i \omega^2}{1 + (\lambda_i \omega)^2} \quad (5)$$

$$G'' = \sum_{i=1}^n \frac{\eta_i \omega}{1 + (\lambda_i \omega)^2} \quad (6)$$

A satisfactory fit was produced with five modes; the relaxation times, λ_i , and viscosities, η_i , associated with each mode are given in Table 1. The model predictions

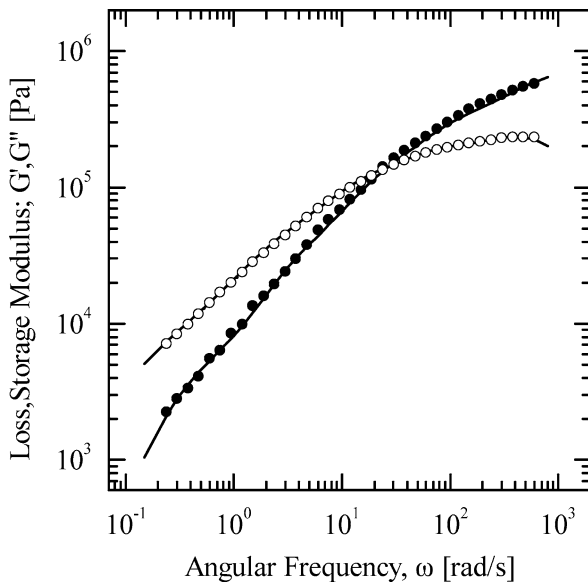


Fig. 4 Small amplitude oscillatory shear rheology of EG8100 at $T_{\text{ref}} = 140 \text{ }^\circ\text{C}$. The data include: loss modulus G'' (unfilled circles), storage modulus G' (filled circles), and fits to a multimode Maxwell model (solid line), the parameters of which are listed in Table 1

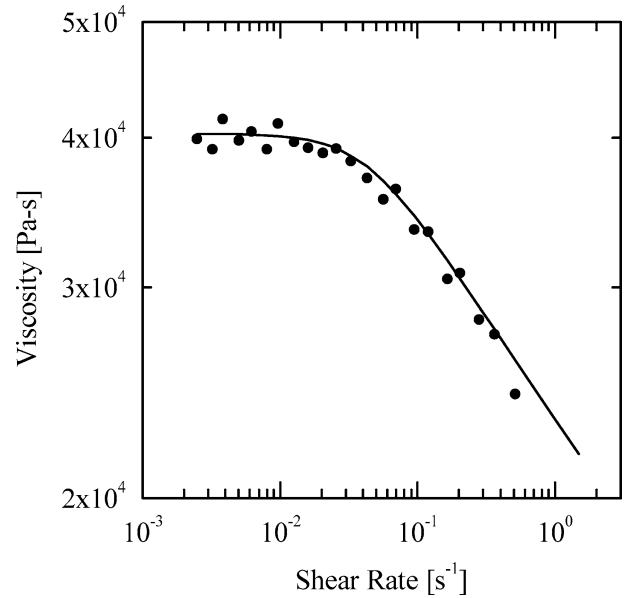


Fig. 5 Steady shear rheology of EG8100 at $T_{\text{ref}} = 140 \text{ }^\circ\text{C}$. The data include viscosity measurements (circles) and a fit to a Carreau model (line)

are superimposed over the data in Fig. 4. For polymer melts, a shear-rate dependent relaxation time can be calculated from viscometric properties of the fluid (Rothstein and McKinley 1999), and an average or Oldroyd relaxation time can be determined through a viscosity weighted average of the relaxation time spectrum,

$$\bar{\lambda} = \frac{\Psi_{10}}{2\eta_0} = \frac{\sum_{i=1}^{N_m} \eta_i \lambda_i}{\sum_{i=1}^{N_m} \eta_i} = 1.52 \text{ s} \quad (7)$$

Shifting of the linear viscoelasticity data over a range of temperatures using the Arrhenius form of the time-temperature superposition shift factor allowed for the determination of the activation energy, $\Delta H/R = 3460 \text{ K}$, which was used in later calculations. The results from fitting the steady shear viscosity data at a reference temperature of $140 \text{ }^\circ\text{C}$ with a Carreau model (Bird et al 1987) are superimposed over the data in Fig. 5. Using this model,

$$\frac{\eta - \eta_\infty}{\eta_0 - \eta_\infty} = \left[1 + (\tau_c \dot{\gamma})^2 \right]^{\frac{n-1}{2}} \quad (8)$$

resulted in a zero-shear rate viscosity of $\eta_0 = 4.0 \times 10^4 \text{ Pa s}$, an infinite-shear rate viscosity of $\eta_\infty = 0$, a time constant for the onset of shear thinning of $\tau_c = 24 \text{ s}$, and a power law exponent of $n = 0.83$. The Carreau model predictions are in good agreement with the viscosity measurements over the entire range of shear rates.

Table 1 Spectrum of relaxation times and moduli

Relaxation time λ (s)	Viscosity η (Pa)
1.98×10^{-3}	3.94×10^5
1.24×10^{-2}	2.11×10^5
5.64×10^{-2}	1.19×10^5
0.327	3.24×10^4
3.22	5.07×10^3

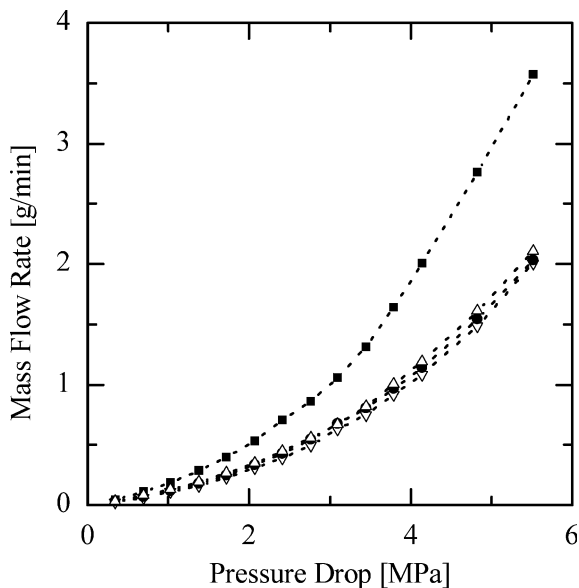


Fig. 6 Flow curves showing effects of bulk temperature versus die heating/cooling. The data include $T_{\text{bulk}} = T_{\text{die}} = 160$ °C (squares), $T_{\text{bulk}} = T_{\text{die}} = 140$ °C (circles), die heating $T_{\text{bulk}} = 140$ °C/ $T_{\text{die}} = 160$ °C (triangles), and $T_{\text{bulk}} = 140$ °C/ $T_{\text{die}} = 130$ °C (upside-down triangles)

Experimental protocol

The extruder was initially calibrated by generating flow curves, several of which will be presented in the following sections. Pressure drop, controlled via the regulator on the nitrogen tank, was ramped up while the mass flow rate of extruded polymer was measured. The latter was done by weighing timed samples of extrudate, using an accurate balance with a sensitivity of 0.001 g (Mettler AC100), collected at a constant pressure drop. Flow curves were generated at various temperature conditions, where bulk temperature is controlled in Zones 2 and 3, and die heating or cooling is done with precise control at Zone 1. We will show through temperature measurements that this precise control affects only a very small portion of the polymer melt near the capillary wall as it exits the die.

Temperature profile measurements of the extrudate were performed using a micro-positioning stage adapted to hold a K-type thermocouple junction at the end of a horizontally-oriented protection tube. The exposed

junction was marched across the exit plane of the capillary die. The center of the thermocouple junction was aligned to be tangent with the exit plane of the capillary, resulting in no upstream effects within the capillary but still capturing the temperature of the extrudate directly at the exit plane. The thermocouple junction had a diameter of $D_{\text{tc}} = 0.35$ mm, resulting in a spatially-averaged temperature measurement of the polymer melt. These measurements are invasive and, although great care is taken during positioning so that the effect is completely downstream of the die exit plane, they can affect the flow as we are trying to measure it. Future experiments are planned with a non-invasive temperature measurement technique such as the Dual Emission Laser Induced Fluorescence (DELIF), described in Coppeta and Rogers (1998). These temperature measurements served to confirm the thermal gradient between the extrudate centerline and wall temperature.

Qualitative flow visualization of the extrudate upon exiting the die was done using a CCD camera (Hitachi KP-M22 N) and video zoom microscope lens with an increased depth of field (Edmund VZM 450i). Quantitative characterization of the extrudate surface showing the sharkskin instability was done optically. Still images of cooled extrudate samples were taken from frames captured with a CCD camera mated to a microscope (Olympus Vanox-T). Using backlighting, the profile of the extrudate was captured and processed using an edge detection routine we developed in MATLAB. The routine utilized a max/min function and fast-Fourier transform to calculate the average amplitude and dominant wavelength of the nearly periodic sharkskin profile.

Results and discussion

Flow curves and effects of die heating

We begin our study of thermal modification by acquiring flow curves at various bulk temperatures, as well as die heating and cooling conditions. In Fig. 6, the effect of changing the bulk material temperature and comparative lack of effect through die heating or cooling is shown. In the figure, the difference in material properties resulting from a 20 °C bulk temperature difference is evident by the increased flow rate for a given applied pressure drop. As the bulk temperature is increased from $T_{\text{bulk}} = 140$ °C to 160 °C, the viscosity, calculated using the Arrhenius form of time-temperature superposition for zero-shear, is reduced from $\eta_0 = 4.0 \times 10^4$ Pa s to $\eta_0 = 2.7 \times 10^4$ Pa s. This 32% decrease in viscosity results in an average 58% increase in mass flow rate, \dot{m} , at a given pressure drop, ΔP . This agrees well with the observations of Pudjijanto and Denn (1994). They found that during stable polymer melt extrusion, the wall shear

stress, $\tau_{\text{wall}} = \Delta P(D/4L)$, increased as $\tau_{\text{wall}} \propto \dot{\gamma}_{\text{app}}^{0.69}$, where the nominal uncorrected value of the apparent shear rate is $\dot{\gamma}_{\text{app}} = 8\bar{V}/D$. Here, $4\dot{m}/\rho\pi D^2$ is the average velocity calculated from the measured mass flow rate. From the experimental observations of Pudjijanto and Denn (1994), we would expect a 59% increase in the observed mass flow rate. In contrast to changing the bulk temperature, the addition of die heating or cooling to the experiment at $T_{\text{bulk}} = 140$ °C produces a negligible effect on the flow curve. Therefore, although the die is being heated to $T_{\text{die}} = 160$ °C or cooled to $T_{\text{die}} = 130$ °C, these experiments clearly show that only the very outermost polymer melt in the die is being heated or cooled beyond the centerline temperature while the bulk properties of the fluid remain unaffected. These qualitative observations of the localization of our thermal modifications will be reinforced with precise temperature profile measurements.

Utilizing the fact that extruded polyethylene becomes cloudy, or experiences loss of gloss as it transitions to sharkskin, the flow curves can be used to explore the onset of the instability. By qualitatively selecting a critical onset point, the data can be separated into stable and unstable flow regimes. When the data are plotted on a log-log scale, they demonstrate a clear transition in slope upon onset of the surface instability, as seen in Fig. 7. Initially, the wall shear stress is found from our experiments to increase as $\tau_{\text{wall}} \propto \dot{\gamma}_{\text{app}}^{0.7}$, independently of bulk or wall temperature. However, a clear transition occurs in the data at larger shear rates and the wall shear

stress is found to increase as $\tau_{\text{wall}} \propto \dot{\gamma}_{\text{app}}^{0.5}$, again, independently of wall or bulk temperature. This change of slope coincides precisely with the loss of gloss of the filament and the transition from the stable flow regime to the sharkskin instability. A similar transition was observed by Pudjijanto and Denn (1994) and our experimentally-measured slopes are in good agreement with the values reported in their work. It should be noted that the onset of sharkskin to this point is assessed in a qualitative manner. As we will discuss below, in order to quantify the effectiveness of die heating or cooling, an exacting procedure must be developed to determine the character of the sharkskin instability.

In addition to showing a clear change in slope at the onset of the sharkskin instability, the data in Fig. 7 strongly supports our original hypothesis that the sharkskin instability can be suppressed through controlled die heating. The three curves shown are extrusion at $T_{\text{bulk}} = 140$ °C with no die heating, $T_{\text{bulk}} = 140$ °C with die heating to $T_{\text{die}} = 160$ °C, and $T_{\text{bulk}} = 160$ °C with no die heating. It should be noted that no die heating means that the die was controlled at the same temperature as the selected bulk. As in the previous flow curves, the curves for $T_{\text{bulk}} = 140$ °C with and without die heating are uniform in terms of stress and shear rate trends. However, the onset point of sharkskin has been suppressed to the next higher experimentally imposed stress level. By heating only the final die exit to $T_{\text{die}} = 160$ °C while keeping the bulk temperature at $T_{\text{bulk}} = 140$ °C, the critical shear stress for the onset of the sharkskin instability from Fig. 7, $\tau_{\text{crit}} = 0.138$ MPa, is found to be consistent with the value observed for the experiments where both the bulk and die were heated to $T_{\text{bulk}} = T_{\text{die}} = 160$ °C, albeit at a lower output rate.

In order to quantify the effects of die heating on the polymer melt, temperature measurements were taken at the die exit. In Fig. 8, profiles taken at a bulk temperature of $T_{\text{bulk}} = 140$ °C with die heating to $T_{\text{die}} = 160$ °C at several increasing output rates are shown. The data do not continue to the die exit ($r = 1.0$ mm) due to the offset caused by the size of the thermocouple junction, $D_{\text{tc}} = 0.35$ mm, in relation to the capillary with diameter, $D = 2$ mm. As a result of the thermocouple junction being fully submerged in the extrudate at the outermost reading, this offset roughly corresponds to one radius, $R_{\text{tc}} = 0.18$ mm. The measurements correspond to average temperatures across the thermocouple junction which is carefully traversed through the extrudate, tangent to the exit plane of the die. A rough extrapolation of the temperature profiles to the edge of the polymer melt extrudate results in a wall temperature of very close to the applied $T_{\text{die}} = 160$ °C. At low output rates and small Peclet numbers, the polymer melt has a long enough residence time in the capillary to be heated to the elevated temperature across the entire profile. As the output rate increases and residence time decreases, a

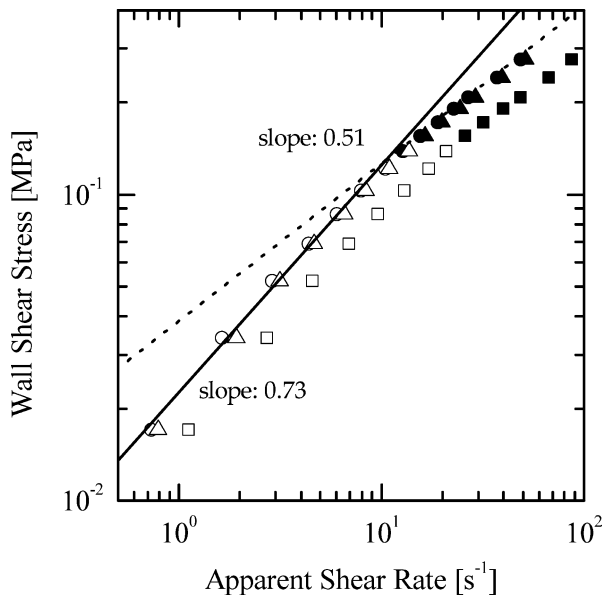


Fig. 7 Flow curves showing transition from stable (open symbols) to unstable sharkskin (closed symbols) extrudate. The data include: $T_{\text{bulk}} = T_{\text{die}} = 140$ °C (circles), $T_{\text{bulk}} = 140$ °C/ $T_{\text{die}} = 160$ °C (triangles), and $T_{\text{bulk}} = T_{\text{die}} = 160$ °C (squares)

strong temperature gradient develops, isolated near the die wall, and less heat is transferred into the polymer. These results illustrate the dependence of the thermal boundary layer thickness on average velocity, as referred to in the dimensionless Peclet number scaling argument presented previously in Eq. 2. The highest flow rate seen in Fig. 8, $\dot{m} = 1.2$ g/min, is equivalent to an average velocity of $\bar{V} = 7.2 \times 10^{-3}$ m/s, and using Eq. 2 results in a Peclet number of $Pe = 376$ corresponding to a thermal boundary layer thickness of approximately 26% of the capillary diameter. Using Eq. 3 gives a Nahme number of $Na = 0.075$, indicating that effects from viscous heating are very small. Close inspection of Fig. 8 shows a small bump in the data near the midpoint of the radius that could be the result of viscous heating, but this occurs only for the highest flow rate shown. In lieu of a more precise and non-invasive temperature measurements, we can conclude that the stated goal of imposing large temperature gradients on the polymer melt extrudate has been attained.

Characterization of sharkskin

A still image of an extrudate in profile exhibiting highly developed sharkskin is shown in Fig. 9. This image illustrates the parameters we will be using to discuss the nearly periodic nature of the sharkskin instability. Qualitative visual inspection of extrudate surfaces indicated that sharkskin amplitude and wavelength both increased as output rate increased. The nature of the surface variations was quantified by analyzing images

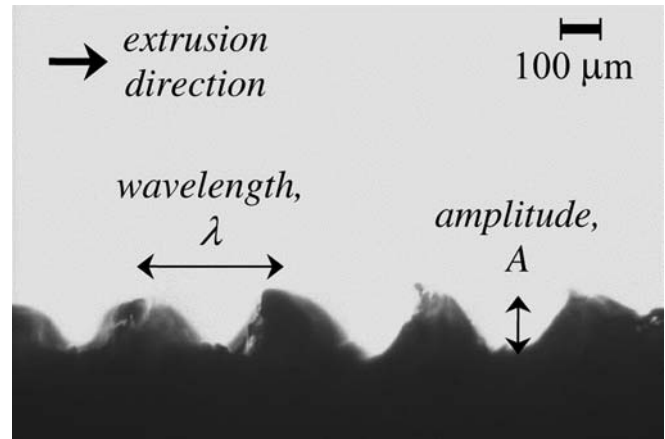


Fig. 9 Characteristic profile photo of EG8100 extrudate with fully developed sharkskin surface

from a wide range of output rates and heating conditions. The resulting plot, seen in Fig. 10, is a quantitative processing map of the sharkskin instability. Looking at the instability in terms of the amplitude of the surface roughness, A , there is a clear exponential growth as output rate increases. Furthermore, throughout the range of die heating and cooling conditions tested, this growth rate appears to be consistent. A specific scaling will be discussed in a later section. Preliminary fitting of the data is included in Fig. 10 to illustrate uniformity of

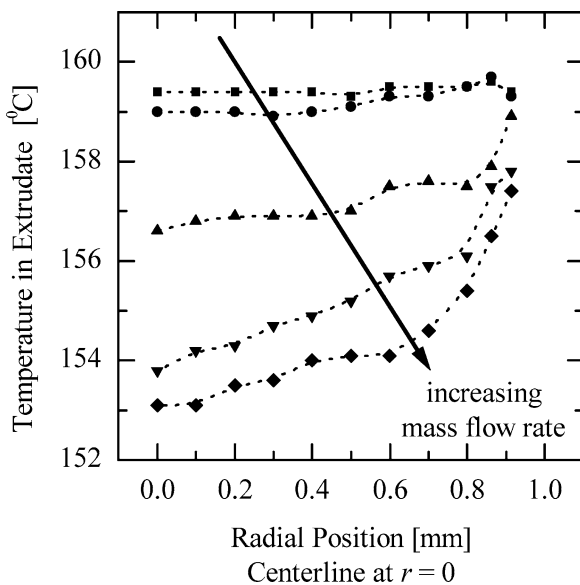


Fig. 8 Radial temperature profiles through extrudate across die exit plane for several increasing mass flow rates, from $\dot{m} = 0.079$ g/min to $\dot{m} = 1.2$ g/min

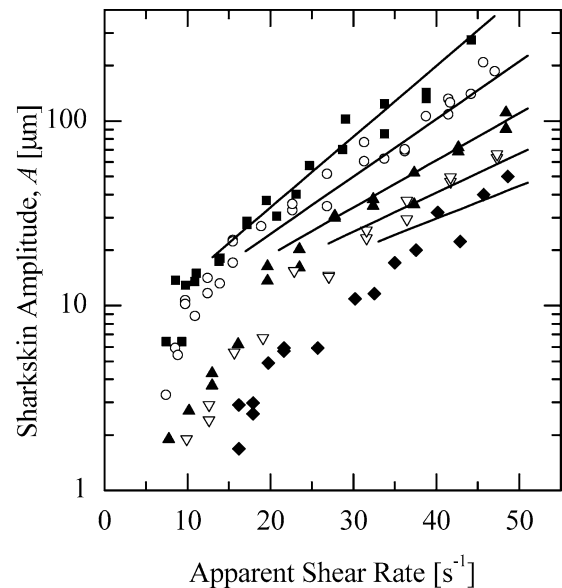


Fig. 10 Sharkskin amplitude as a function of shear rate at various die heating or cooling conditions, a quantitative processing map. All curves are at $T_{\text{bulk}} = 140$ °C with die heating/cooling. The data include $T_{\text{die}} = 130$ °C (squares), $T_{\text{die}} = 140$ °C (circles), $T_{\text{die}} = 150$ °C (filled triangles), $T_{\text{die}} = 160$ °C (unfilled triangles), and $T_{\text{die}} = 170$ °C (diamonds). Exponential fits included and addressed in Fig. 14

the data between temperature conditions in the given window. This scaling suggests that the consistent fit is valid for shear rates far from the onset conditions of sharkskin; the initial growth from submicron roughness and smooth surfaces to sharkskin is much stronger. The scatter in the data is due primarily to the $1\ \mu\text{m}$ resolution of the images used.

An additional feature of the data in Fig. 10 is the lack of hysteresis, explored in a series of experiments performed to determine the nature of the instability. The shear rate at which the polymer was extruded was initially ramped up and then back down. Samples of the extrudate were collected along both paths of the flow curve. The resulting measurements of the amplitude of the surface roughness demonstrated no significant deviation indicative of hysteresis. This result suggests that the sharkskin instability is a supercritical bifurcation (Iooss and Joseph 1980). Our work contradicts the results of Bertola et al (2003) and Meulenbroek et al (2003), who investigated the extrusion of a polyvinyl alcohol sodium tetraborate solution and found the amplitude growth of the sharkskin instability was hysteretic with shear rate. Based on the results of their experiments and the stability analysis of Meulenbroek et al (2003), Bertola et al (2003) claim that there is one fundamental intrinsic route to the sharkskin instability and that the instability has the characteristics of a weakly subcritical bifurcation. The origin of this discrepancy in our experiments is unclear and, to our knowledge, no other source indicates that sharkskin has the characteristics of a subcritical bifurcation.

There is a need to quantify the onset conditions of the sharkskin instability. Rather than qualitatively assigning a surface as stable or unstable based on its “by eye” visual appearance, the map shown in Fig. 10 allows a specific characteristic amplitude to be designated as the condition for the onset of the sharkskin instability. The quantitative map encompasses the region of processing at the point where some level of instability is already present. This is due to the fact that the optical edge detection routine has difficulty processing amplitudes smaller than about $1\ \mu\text{m}$. Sharkskin has historically been identified as a loss of gloss on the surface of the extrudate. Based on our qualitative inspection, this corresponds to a surface roughness of approximately $A \approx 10\ \mu\text{m}$. If a vertical slice is taken through the data, thereby holding the shear rate fixed, the amplitude is found to decrease as the degree of die heating is increased. This can be seen explicitly in the series of images presented in Fig. 11. These images show a decrease in surface roughness from $A = 90\ \mu\text{m}$ to $25\ \mu\text{m}$ to $9\ \mu\text{m}$ as the capillary die wall temperature is decreased from $T_{\text{die}} = 170\ \text{°C}$ to $150\ \text{°C}$ to $130\ \text{°C}$ at a shear rate of $\dot{\gamma} = 30\ \text{s}^{-1}$ and a bulk temperature of $T_{\text{bulk}} = 140\ \text{°C}$. Therefore, a surface temperature

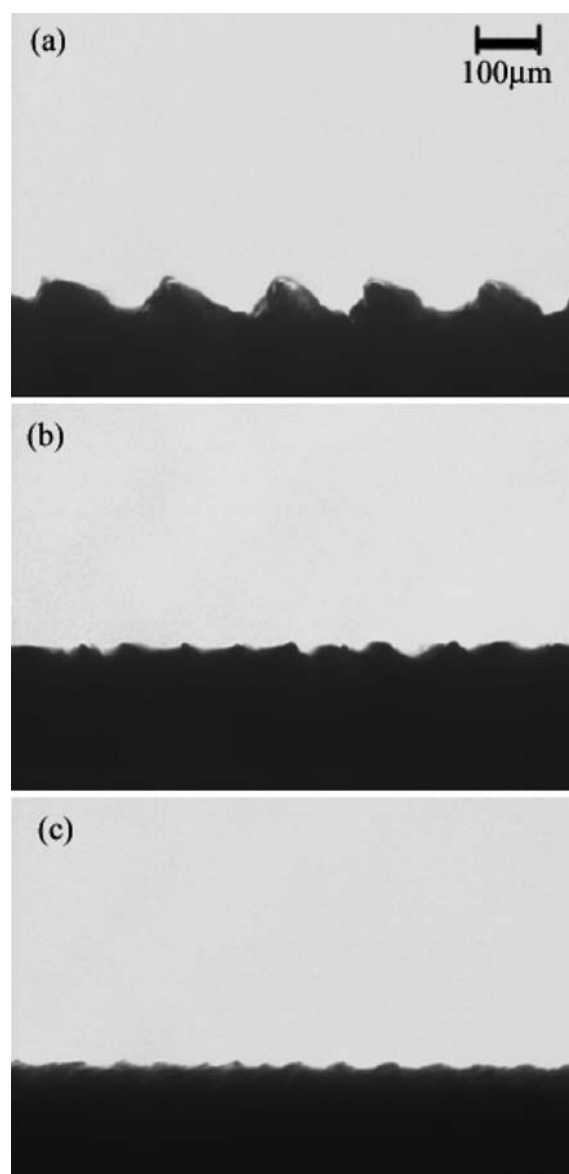


Fig. 11 Succession of profile photos at constant apparent shear rate of $\dot{\gamma} = 30\ \text{s}^{-1}$ and a constant bulk temperature of $T_{\text{bulk}} = 140\ \text{°C}$ with increasing die temperature. The data include **a** $T_{\text{die}} = 130\ \text{°C}$, **b** $T_{\text{die}} = 150\ \text{°C}$, and **c** $T_{\text{die}} = 170\ \text{°C}$

modification of $40\ \text{°C}$ about the bulk temperature produces an order of magnitude difference in the measured sharkskin amplitude. Alternatively, a given amplitude can be selected and a horizontal slice taken through the data in Fig. 10. We observe that modification of the die temperature by $40\ \text{°C}$ through localized heating or cooling makes it possible to change the output rates required to achieve a desired surface roughness by a factor of three. The implications of this quantitative surface roughness map over a given processing region are broader than simply suppressing sharkskin to higher output levels or eliminating it

entirely at a specific condition, flow rate, or pressure drop. Through the use of controlled die heating, the polymer melt extrudate can be processed at a selected operating condition in terms of stress and shear levels, allowing one to “dial in” a specific amplitude and impart a desired functionality to the surface.

Mechanism of sharkskin

The effectiveness of isolated heating at the die wall gives some insight into the mechanism of the sharkskin instability. Our results lend support to the theory that sharkskin originates in the interaction of the polymer with the die wall and local stresses at the die exit. To further quantify this dependence, a local Deborah and Weissenberg number are formed based on the conditions at the capillary die wall:

$$De_{\text{local}} = \lambda(T_{\text{die}})f \quad (9)$$

$$Wi_{\text{local}} = \lambda(T_{\text{die}})\dot{\gamma}_{\text{app}} \quad (10)$$

where f is the frequency of the sharkskin instability. For these calculations, the relaxation time at the wall, $\lambda(T_{\text{die}})$, was evaluated using the Arrhenius form of the time-temperature superposition shift factor, Eq. 1. The Deborah and Weissenberg numbers describe the ratios of the characteristic fluid relaxation time to the characteristic time scale of the flow, and the shear rate, respectively. The two dimensionless quantities also differ in that the Deborah number is used for a time-dependent flow, and Weissenberg for steady flow, as defined by Morrison (2001). In Fig. 12, two vertical slices of the data in Fig. 10, holding the apparent shear rate constant at $\dot{\gamma} = 15 \text{ s}^{-1}$ and $\dot{\gamma} = 30 \text{ s}^{-1}$, are recast in terms of the local Deborah number. As the wall temperature increases, the frequency of the instability increases. When the frequency of the instability is non-dimensionalized by the relaxation time at the die wall to form the local Deborah number, however, the data are found to collapse to a single constant value of $De \approx 38$ for $\dot{\gamma} = 15 \text{ s}^{-1}$ and $De \approx 50$ for $\dot{\gamma} = 30 \text{ s}^{-1}$, independent of die temperature. Similarly, if the amplitude is held fixed by taking a horizontal slice of Fig. 10, the shear rate required to achieve a given surface roughness can be determined for various die temperatures. The data in Fig. 13, for amplitudes of $A = 20 \text{ }\mu\text{m}$ and $A = 30 \text{ }\mu\text{m}$, show that the apparent shear rate required to achieve a given surface instability amplitude increases with wall temperature. If the shear rate data is non-dimensionalized, the local Weissenberg number is found to remain nearly constant, $Wi \approx 32$ for $A = 20 \text{ }\mu\text{m}$ and $Wi \approx 37$ for $A = 30 \text{ }\mu\text{m}$, independent of die temperature. From these observations, we can conclude that the sharkskin instability is independent of the viscometric bulk fluid properties and only a function of the rheological properties of the fluid

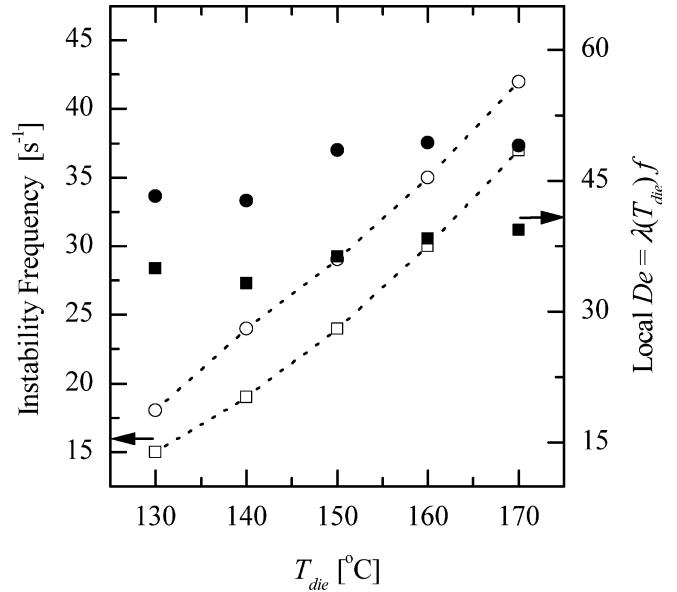


Fig. 12 Sharkskin frequency and local Deborah number at die wall as a function of die temperature for fixed apparent shear rate (a vertical slice of Fig. 10). The data include, for $\dot{\gamma} = 15 \text{ s}^{-1}$: local De (filled squares), and frequency (unfilled squares); for $\dot{\gamma} = 30 \text{ s}^{-1}$: local De (filled circles), and frequency (unfilled circles)

closest to the die wall and the levels of stress due to both viscous and elastic effects resulting from the enormous deformation of the fluid near the stress singularity.

To further demonstrate this conclusion, all of the data from the quantitative map in Fig. 10 can be collapsed onto a single master flow curve by plotting the sharkskin amplitude as a function of the local Weissenberg number in Fig. 14. Within the limits of experimental error, the data agree very well. The use of this dimensionless quantity now becomes even more insightful. When an exponential fit is applied to the master curve, it becomes clear that there is some critical Weissenberg number ($Wi_{\text{local}} \approx 20$) at which there is a transition in the growth rate of the amplitude data. Fitting the data well above the onset conditions ($A > 10 \text{ }\mu\text{m}$) for the sharkskin instability gives a scaling of $A = 5.8e^{0.047Wi}$; rewritten in terms of apparent shear rate, this same scaling was also applied to the data in Fig. 10 and the results are quite good.

As discussed in the previous section, the absence of hysteresis in the data suggests the transition from a smooth extrudate to the sharkskin instability is a supercritical Hopf bifurcation. An expression for both the amplitude of the surface roughness and the frequency of the instability at Weissenberg numbers above and close to the onset of the instability can be determined from the following asymptotic results for supercritical Hopf bifurcations (Iooss and Joseph 1980)

$$A = A_0(Wi_{\text{local}} - Wi_{\text{crit}})^{1/2} \quad (11)$$

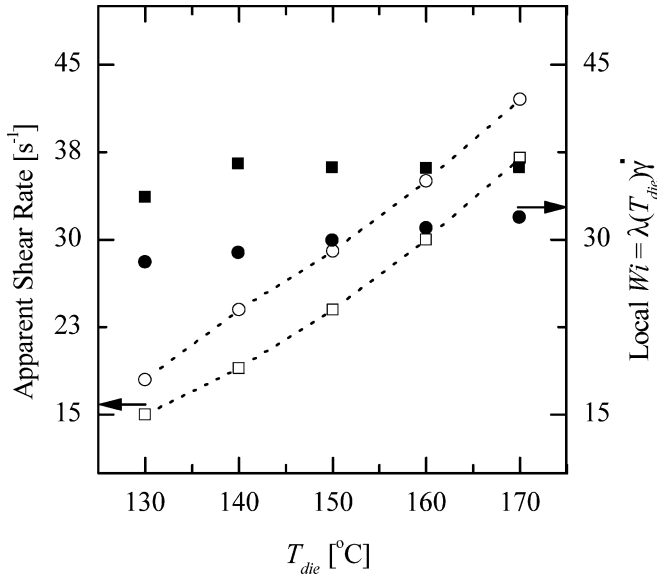


Fig. 13 Apparent shear rate and local Weissenberg number at die wall as a function of die temperature for a fixed sharkskin amplitude (a horizontal slice of Fig. 10). The data include, for $A=20\ \mu\text{m}$: local Wi (filled squares), and apparent shear rate (unfilled squares); for $A=30\ \mu\text{m}$, local Wi (filled circles), and apparent shear rate (unfilled circles)

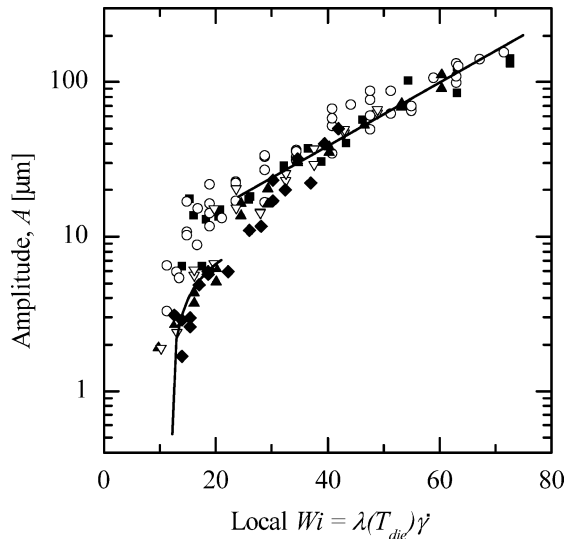


Fig. 14 Master curve of all amplitude data at the same bulk/die temperature conditions as for Fig. 10, using the local Weissenberg number. Fits are included for data near and far from onset of sharkskin instability, $A=2.4(Wi-12)^{1/2}$ and $A=5.8e^{0.047Wi}$, respectively

$$f = c_1 + c_2(Wi_{\text{local}} - Wi_{\text{crit}})^{1/2} \quad (12)$$

where Wi_{crit} is the critical Weissenberg number for the onset of the sharkskin instability and A_0 , c_1 , and c_2 are constants. A good fit over all the low Weissenberg number amplitude data ($A < 10\ \mu\text{m}$) in Fig. 14 was achieved using Eq. 11 and the following parameters:

$A_0=2.4\ \mu\text{m}$ and $Wi_{\text{crit}}=12$. These results lend further support to the classification of this instability as supercritical. In addition, this critical Weissenberg number is in good agreement with values reported in the literature (Meulenbroek et al 2003). As seen in Fig. 14, the initial deviations from a smooth extrudate appear to be well described by the linear theory. However, when $Wi_{\text{local}} \gg Wi_{\text{crit}}$, nonlinear dynamics begin to dominate the flow kinematics and the growth in the amplitude data transitions to the exponential growth regime described previously.

To investigate the role of temperature gradients near the die wall, a final set of experiments were performed. The temperature at the die wall was set to $T_{\text{die}}=150\ \text{°C}$ and bulk temperature was varied from $T_{\text{bulk}}=130\ \text{°C}$ to $170\ \text{°C}$. Starting with the lowest bulk temperature, output rate was increased to slightly above the point of sharkskin onset. The mass flow rate was recorded and samples were taken for analysis. Pressure was released, bulk temperature increased, and after an equilibration period, the output rate was gradually increased until the same mass output rate was attained at the new temperature conditions. The pressure-controlled extruder was adjusted manually for output rates and resulted in an error of approximately 1% about the average. Figure 15 shows the distribution of data taken at $5\ \text{°C}$ increments with several samples taken at each increment. Although there is some scatter in the data, which can be attributed to the inherent error in the graphical analysis method at these small amplitudes, the trend in the amplitude is nearly constant with an average value of approximately

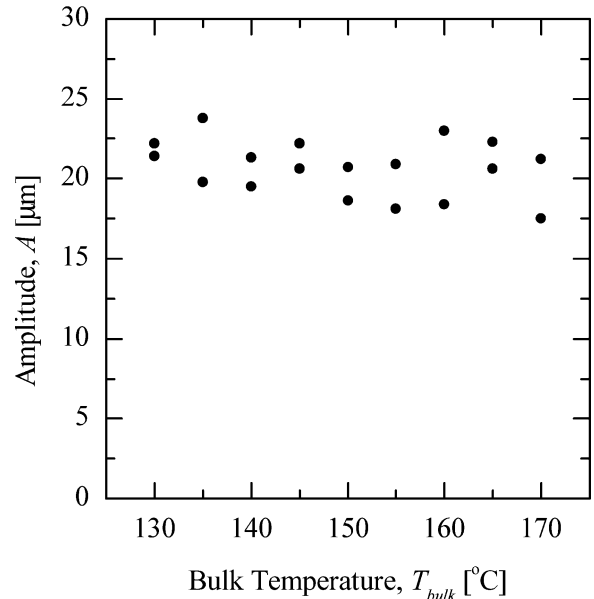


Fig. 15 Sharkskin amplitude at constant mass flow rate $\dot{m}=0.95\ \text{g/min}$, as a function of bulk temperature for a fixed wall temperature, $T_{\text{wall}}=150\ \text{°C}$

$A = 20 \mu\text{m}$. These experiments demonstrate that the character of the sharkskin amplitude remains constant in the presence of changing temperature gradients and is a function only of the actual temperature at the die wall.

Conclusions

Precise and localized die heating has been shown to suppress the onset of the sharkskin surface instability in the extrusion of LLDPE. Sharkskin has also been quantitatively characterized as a function of the processing conditions, showing that the severity of the distortions grows with an exponential trend with increasing apparent shear rate at all die heating conditions. The resulting quantitative processing map for sharkskin amplitude is a useful tool that allows for the precise control of sharkskin surface distortions through the modification of die wall temperature. Analysis of the same quantitative map gives fundamental support to the mechanism of sharkskin being inherent in conditions at the die wall, and nearly independent of conditions in the bulk.

These results have some interesting practical implications to the extrusion of LLDPE and other polymers

that exhibit the sharkskin instability. Bulk processing temperatures can be much lower than those needed to suppress the instability. The heating of a very small portion of the die at the exit provides the same benefit as processing the entire bulk at that higher temperature. Bulk processes can be cooler and more energy efficient, while cooling times of the polymer melt extrudate are minimized. Precise control of sharkskin as alluded to in the preceding experimental results leads to future theoretical applications such as the extrusion of products with specifically designed or even varying surface roughness. In film blowing or sheet extrusion, inner and outer dies could produce surfaces smooth on one side and rough on the other. On a qualitative level, Rutgers et al (2002) have already stated that temperature gradients between the inner and outer die lips in a film blowing application produce smooth and sharkskin surfaces on the respective surfaces of a bubble. Further development of temperature control systems could result in dies that would respond quickly and could pattern surfaces as they were extruded.

Acknowledgements The authors would like to acknowledge the Executive Area for Research for partial support of this research through a Healy Endowment Grant.

References

- Barone JR, Plucktaveesak N, Wang SQ (1998) Interfacial molecular instability mechanism for sharkskin phenomenon in capillary extrusion of linear polyethylenes. *J Rheol* 42:813–832
- Bertola V, Meulenbroek B, Wagner C, Storm C, Morozov A, Saarloos Wv, Bonn D (2003) Experimental evidence for an intrinsic route to polymer melt fracture phenomena: A nonlinear instability of viscoelastic Poiseuille flow. *Phys Rev Lett* 90:114502(4)
- Bird RB, Armstrong BC, Hassager O (1987) Dynamics of polymeric liquids: Vol 1: Fluid mechanics. Wiley, New York
- Chung CI (2000) Extrusion of polymers: theory and practice. Carl Hanser, Munich, Germany
- Cogswell FN (1976) A method for reducing sharkskin on extruded polymeric material. British Patent #1 441 586
- Cogswell FN (1977) Stretching flow instabilities at the exits of extrusion dies. *J Non-Newton Fluid* 2:37–47
- Coppeta J, Rogers C (1998) Dual emission laser induced fluorescence for direct planar scalar behavior measurements. *Exp Fluids* 25:1–15
- Denn MM (2001) Extrusion instabilities and wall slip. *Annu Rev Fluid Mech* 33:265–287
- Dhori PK, Jeyaseelan RS, Giacomini AJ, Slattery JC (1997) Common line motion III: implication in polymer extrusion. *J Non-Newton Fluid* 71:231–243
- El Kissi N, Piau J-M (1994) Adhesion of linear low density polyethylene for flow regimes with sharkskin. *J Rheol* 38:1447–1463
- Ghanta VG, Riise BL, Denn MM (1998) Disappearance of extrusion instabilities in brass capillary dies. *J Rheol* 43:435–442
- Howells ER, Benbow JJ (1962) Flow defects in polymer melts. *T J Plast I* 30:240–253
- Inn YW, Fisher RJ, Shaw MT (1998) Visual observation of development of sharkskin melt fracture in polybutadiene extrusion. *Rheol Acta* 37:573–582
- Iooss G, Joseph D (1980) Elementary stability and bifurcation theory. Springer, Berlin Heidelberg New York
- Kalika DS, Denn MM (1987) Wall slip and extrudate distortion in linear low-density polyethylene. *J Rheol* 31:815–834
- Larson RG (1992) Instabilities in viscoelastic flows. *Rheol Acta* 31:213–263
- Mackley M, Rutgers R, Gilbert D (1998) Surface instabilities during the extrusion of linear low density polyethylene. *J Non-Newton Fluid* 76:281–297
- Meulenbroek B, Storm C, Bertola V, Wagner C, Bonn D, Saarloos Wv (2003) Intrinsic route to melt fracture in polymer extrusion: A weakly nonlinear subcritical instability in viscoelastic Poiseuille flow. *Phys Rev Lett* 90:024502(4)
- Mhetar V, Archer LA (1998) Slip in entangled polymer melts. 1. General features. *Macromolecules* 31:8607–8616
- Michaeli W (1984) Extrusion dies: design and engineering computations. Carl Hanser/Macmillan, Munich, Germany
- Migler KB, Lavalee C, Dillon MP, Woods SS, Gettinger CL (2001) Visualizing the elimination of sharkskin through fluoropolymer additives: Coating and polymer-polymer slippage. *J Rheol* 45:565–581
- Morrison FA (2001) Understanding rheology. Oxford University Press, New York

-
- Perez-Gonzalez J, Denn MM (2001) Flow enhancement in the continuous extrusion of linear low-density polyethylene. *Ind Eng Chem Res* 40:4309–4316
- Petrie CJS, Denn MM (1976) Instabilities in polymer processing. *AIChE J* 22:209–236
- Piau JM, El Kissi N, Tremblay B (1989) Influence of upstream instabilities and wall slip on melt fracture and sharkskin phenomena during silicones extrusion through orifice dies. *J Non-Newton Fluid* 34:145–180
- Piau J-M, Kissi NE, Toussant F, Mezghani A (1995) Distortion of polymer melt extrudates and their elimination using slippery surfaces. *Rheol Acta* 34:40–57
- Pudjijanto S, Denn MM (1994) A stable “island” in the slip-stick region of linear low-density polyethylene. *J Rheol* 38:1735–1744
- Ramamurthy AV (1986) Wall slip in viscous fluids and influence of materials of construction. *J Rheol* 30:337–357
- Rothstein JP, McKinley GH (1999) Extensional flow of a polystyrene Boger fluid through a 4:1:4 axisymmetric contraction/expansion. *J Non-Newton Fluid* 86:61–88
- Rutgers R, Clemeur N, Husny J (2002) The prediction of sharkskin instability observed during film blowing. *Int Polym Proc* 17:214–222
- Santamaria A, Fernandez M, Sanz E, Lafuente P, Munoz-Escalona A (2003) Postponing sharkskin of metallocene polyethylenes at low temperatures: the effect of molecular parameters. *Polymer* 44:2473–2480
- Tordella JP (1963) Unstable flow of molten polymers: A second site of melt fracture. *J Appl Polym Sci* 7:215–229
- Touloukian YS (1979) Thermophysical properties of matter; the TPRC data series. IFI/Plenum, New York
- Winter HH (1977) Viscous dissipation in shear flows of molten polymers. *Adv Heat Transfer* 13:205–267